# Exposure to the gut microbiota from cigarette smoke-exposed mice exacerbates cigarette smoke extract-induced inflammation in zebrafish larvae

Simone Morris[1]†, Kathryn Wright[1], Vamshikrishna Malyla[2,3], Warwick J Britton[1,4], Philip M Hansbro[2], Pradeep Manuneedhi Cholan[1] *†, Stefan H Oehlers[1,5] *

Affiliations
1 Tuberculosis Research Program at the Centenary Institute, The University of Sydney, Camperdown, NSW, Australia.
2 Centre for Inflammation, Centenary Institute and University of Technology Sydney, Faculty of Science, School of Life Sciences, Sydney, NSW, Australia.
3 Discipline of Pharmacy, Graduate School of Health, University of Technology Sydney, Sydney, NSW, Australia.
4 Department of Clinical Immunology, Royal Prince Alfred Hospital, Camperdown, Australia.
5 The University of Sydney, Faculty of Medicine and Health, Camperdown, NSW, Australia
† Co-first authors, contributed equally
* Co-corresponding authors: pradeep.manuneedhicholan@mq.edu.au or s.oehlers@centenary.org.au

**Abstract**
Cigarette smoke (CS)-induced inflammation leads to a range of diseases including chronic obstructive pulmonary disease and cancer. The gut microbiota is a major modifying environmental factor that determine the severity of cigarette smoke-induced pathology. Microbiomes and metabolites from CS-exposed mice exacerbate lung inflammation via the gut-lung axis of shared mucosal immunity in mice but these systems are expensive to establish and analyse. Zebrafish embryos and larvae have been used to model the effects of cigarette smoking on a range of physiological processes and offer an amenable platform for screening modifiers of cigarette smoke-induced pathologies with key features of low cost and rapid visual readouts. Here we exposed zebrafish larvae to cigarette smoke extract (CSE) and characterised a CSE-induced leukocytic inflammatory phenotype with increased neutrophilic and macrophage inflammation in the gut. The CSE-induced phenotype was exacerbated by co-exposure to microbiota from the faeces of CS-exposed mice, but not control mice. Microbiota could be recovered from the gut of zebrafish and studied in isolation in a screening setting. This demonstrates the utility of the zebrafish-CSE exposure platform for identifying environmental modifiers of cigarette smoking-associated pathology and demonstrates that the CS-exposed mouse gut microbiota potentiates the inflammatory effects of CSE across host species.

## Introduction

Smoking tobacco is one of the greatest public health challenges, accounting for more than 8 million deaths worldwide, per year (1). It ranks as the third leading risk factor for illness and death, including from diseases such as cancers and inflammatory disorders like inflammatory bowel disease (IBD) (1-4). Cigarette smoke (CS) contains a multitude of toxic compounds affecting cell function, foetal development, gut function and microbiome, neural activity, inflammation, and lung cancer (3, 5-12).

The toxicity of CS has further been demonstrated to alter the microbiome of smokers, resulting in respiratory and gut microbiome dysbiosis, which in turn is associated with increased peptic ulcers, IBD and gastrointestinal cancers via the gut-lung axis of shared mucosal immunity (3, 4, 6, 11, 13). This is suggested to occur through alterations to the immune system (5), mucin production (6) or through direct anti-microbial effects of the toxins within the smoke (14). Shifts in gut microbiome and the profile of gut metabolites and pathology are associated with chronic obstructive pulmonary disease (COPD) in humans and CS-induced emphysema in mice (4, 10, 11, 15, 16). Microbiomes and metabolites associated with COPD and CS exacerbate lung inflammation via the gut-lung axis of shared mucosal immunity contributing to lung pathology in mammals (4, 11, 17).

Zebrafish have been used to study the developmental defects caused by CS exposure. These studies demonstrated stunted embryonic development upon exposure to cigarette smoke extract (CSE) and smoke condensate (18-20). Exposure of adult zebrafish to CSE reduced the capacity for fin regeneration (19), as well as behavioural abnormalities in response to nicotine (7). A study by Progatzky *et al.* further modelled the respiratory effects of CS using adult zebrafish gills demonstrating increased pro-inflammatory cytokine production and reduced immune cell recruitment (21). Massarsky *et al.* used total particulate matter (TPM) from cigarettes to model the effects of CS in zebrafish, and showed cardiac malfunction and defects in brain vascularisation (22) as well as behavioural alterations (23).

Thus far, the effect of CS exposure on immune function has been unexplored in zebrafish embryos and larvae (19, 21). This transparent stage of development provides the opportunity to investigate the inflammatory effects of CSE by live imaging of fluorescently tagged leukocytes, and is amenable to simplified experimental manipulation by gene editing or treatment with small molecules by immersion (24). Here we define the pro-inflammatory effects of CSE on larval zebrafish and find a transferrable effect of mammalian CS-associated microbiota on CSE-induced inflammation in larval zebrafish.

## Methods

### Zebrafish husbandry

Zebrafish embryos were obtained through natural spawning (Sydney Local Health District Animal Welfare Committee Approval 17-036). The transgenic strains used to visualise leukocytes were *Tg(lyzC:DsRed)*$^{nz50}$, where neutrophils are labelled by DsRed2 expression (25), and *Tg(mfap4:turquoise)*$^{xt27}$, where macrophages are labelled by Turquoise2 (26). Embryos were raised in E3 media supplemented with methylene blue in a dark incubator at 28°C until 1 day post fertilisation (dpf). Cleaned 1 dpf embryos were transferred to E3 without methylene blue and reared (dark incubator, 28°C) until used.

Zebrafish larvae were anaesthetised in 250 µg/mL MS-222 (Tricaine, Sigma) and euthanised either by fixation in 4% paraformaldehyde, lysis in Trizol, or disposed of in bleach as per biosafety protocols.

### Preparation of CSE

Cigarette smoke extract (CSE) was prepared by using a custom-built smoking device where reference cigarette 3R4F (Kentucky Tobacco Research & Development Centre) was lit using a lighter and CS was bubbled directly in to 10 mL of PBS until the whole cigarette was exhausted. This 10 mL of CSE was filtered using a 0.22-micron filter to remove CS-derived debris. This preparation of the smoke of one cigarette per 10 mL PBS is considered 100% CSE and was diluted as indicated. CSE was prepared fresh before treatment.

### Exposure of zebrafish to CSE

Embryos/larvae were exposed to CSE at a density of approximately 1 larva per mL of E3 in plastic Petri dishes at the ages indicated, either 3 or 5 dpf, and maintained in a dark incubator at 28°C. The stock solution of 100% CSE in PBS was diluted directly into E3 zebrafish media to a final concentration of 1%, 2%, or 3%. Filter sterilised PBS was used as vehicle control.

Zebrafish behavioural analysis

Zebrafish larvae were transferred to a 24-well plate with 1 embryo per well in their CSE-supplemented E3 media. The plate was transferred to a ZebraBox (Viewpoint) and locomotion was recorded for 15 minutes. Video files were analysed using EthoVision XT 11 (Noldus) using the following parameters: sensitivity 110, video pixel smoothing low, subject size 4-4065. Locomotion analysis was calculated as the total distance travelled (mm) of individual larva over the recording window.

Tail transection assays

Caudal fin amputations were performed on 5 dpf larvae. Larvae were anesthetised with 2.5% (v/v) ethyl-3-aminobenzoate methanesulfonate (tricaine) (Sigma, E10521), wounded posterior to the notochord using a sterile scalpel and kept in a 28°C incubator to recover as previously described (27). Wounded larvae were imaged at 6 hours post wounding.

Imaging and image analysis

Larvae were imaged using a Leica M205FA fluorescent microscope. ImageJ software was used to quantify fluorescent pixel counts as previously described (27).

Generation of microbiome-depleted zebrafish embryos

Microbiome-depleted zebrafish were created and maintained as previously described (28). Briefly, freshly laid embryos were rinsed with 0.003% v/v bleach in sterile E3 and rinsed 3 times with sterile E3. Bleached embryos were raised in sterile E3 supplemented with 50 µg/mL ampicillin (Sigma), 5 µg/mL kanamycin (Sigma) and 250 ng/mL amphotericin B (Sigma) in sterile tissue culture flasks. Dead embryos and chorions were aseptically removed at 1 and 3 dpf, respectively.

Generation of mouse faecal microbiota specimens

Mice were housed at the Centenary Institute (Sydney Local Health District Animal Welfare Committee Approval 2020-003). C57BL/6J mice were housed in a pathogen-free and temperature-controlled environment, with 12 hours of light and 12 hours of darkness, and free access to food and water. Mice were smoked with 12x 3R4F cigarettes for 75 minutes, twice a day, 5 days per week for 10 weeks by using a custom-designed and purpose-built nose-only, directed flow inhalation and smoke-exposure system (CH Technologies, NJ) (10, 29). This is representative of a pack-a-day smoker (2).

Faecal pellets were collected from mice that were housed in different cages. Individual faecal pellets were collected into sterile 1.7 mL microcentrifuge tubes and homogenised in 1 mL of sterile E3 by pipetting. Homogenised specimens were centrifuged (500 x*g*, 2 minutes) to sediment fibrous material and supernatant were collected then pooled. Pooled supernatants were supplemented with glycerol to a final concentration of 25% v/v, aliquoted, and frozen at -80°C before use.

Mice were not anaesthetised for these procedures and were used for other experiments as per Approval 2020-003 where they were eventually sacrificed by CO2 asphyxiation.

Exposure of zebrafish larvae to mouse faecal microbiota

Microbiome-depleted zebrafish were rinsed at 3 dpf with sterile E3, without antibiotic and amphotericin B supplementation, and colonised by the addition of 200 µL thawed faecal homogenate supernatant into 30 mL sterile E3 delivering a final concentration of ~$5x10^4$ CFU per mL. Enumeration of culturable bacterial load was carried out by culture under aerobic conditions at 28°C on LB agar (Thermofisher).

Detection of gene expression

142 Groups of at least 10 larvae were homogenised in Trizol (Thermofisher) and processed for RNA extraction
143 as per manufacturer's instructions. cDNA was reverse transcribed using the Applied Biosystems High
144 Capacity cDNA synthesis kit (Thermofisher) from 2 µg of total RNA. Quantitative PCR was carried out on a
145 CFX Connect machine (Biorad) with Powerup SYBR reagent (Thermofisher), primer sets were (5'-3'): *il1b* Fw
146 ATCAAACCCCAATCCACAGAGT, Rv GGCACTGAAGACACCACGTT; *18s* Fw TCGCTAGTTGGCATCGTTTATG, Rv
147 CGGAGGTTCGAAGACGATCA.
148
149 Statistical analysis
150 Statistical testing was carried out by ANOVA with post hoc multiple comparisons as appropriate using
151 GraphPad Prism 9 (GraphPad). Data are expressed as mean ± SD, calculated P values are provided in
152 graphs. Outliers were excluded using a 1% robust regression and outlier removal (ROUT) test. Every
153 datapoint represents a single embryo unless otherwise noted as for qPCR analyses.
154
155 **Results**
156 Chronic exposure to CSE is toxic to zebrafish post-hatching larvae
157 To establish a survivable dose of CSE that did not cause gross pathology, we exposed 3 dpf zebrafish larvae
158 to a range of CSE doses and monitored survival. We found exposure at up to 2% CSE was tolerated by
159 zebrafish larvae (Figure 1A), with no overt changes to morphology (Figure 1B). Exposure to 3% CSE caused
160 significant mortality within 1 day post exposure.
161
162 To verify that the CSE was bioactive at 1% and 2% concentrations, we tracked larval motility to detect
163 nicotine-induced increases in motility at 5 dpf, or 2 days post exposure (30). Exposure to 1% or 2% CSE
164 increased the total distance travelled of zebrafish larvae compared to mock exposed larvae in a 15 minute
165 recording period indicating components of the CSE were still bioactive after 2 days of immersion exposure
166 in E3 media (Figure 1C).
167
168 We next used *Tg(lyzC:DsRed)*$^{nz50}$ larvae to visualise neutrophils and *Tg(mfap4:turquoise)*$^{xt27}$ to visualise
169 macrophages (25, 26). Immune cell fluorescent area was used as a proxy to estimate changes to immune
170 cell number by non-invasive live imaging. We performed tail transection on 5 dpf larvae that had been
171 exposed to CSE from 3 dpf and assessed leukocyte recruitment to the wound at 6 hours post wounding.
172 While neutrophil recruitment was slightly but statistically significantly reduced by 1% CSE, there was no
173 effect of 2% CSE exposure compared to vehicle control and overlap between neutrophil recruitment in the
174 1% and 2% CSE exposure groups (Figure 1D). There was significantly more macrophage recruitment to
175 wounds in 2% CSE-exposed larvae compared to control and 1% CSE larvae (Figure 1E).
176
177 Acute exposure to CSE induces myelopoiesis in zebrafish larvae
178 To examine the acute effects of CSE exposure on larvae after major organogenesis is complete, we exposed
179 5 dpf larvae to CSE for 24 hours. Immersion in 1% and 2% CSE caused a gradated increase in total
180 neutrophil fluorescent area in zebrafish larvae compared to PBS vehicle (Figure 2A and 2B). This
181 inflammatory effect of CSE appeared stronger on total macrophage fluorescent area with a statistically
182 significant increase in total macrophages in 2% CSE-exposed compared to control larvae (Figure 2C and 2D).
183
184 Acute exposure to CSE induces an inflammatory response in the gut of zebrafish larvae
185 The effects that we observed suggested that CSE induced an inflammatory haematopoietic response. Since
186 the larval midgut and hindgut is an important site of immune response to chemical irritants, we next
187 quantified leukocyte recruitment to the larval intestine of 6 dpf larvae that had been exposed to 2% CSE
188 from 5 dpf (31). Leukocyte fluorescence was increased in the gut compared to either control or 1% CSE-
189 exposed larvae (Figure 3A and 3B). However, the estimation of gut macrophages by fluorescent pixel count
190 in our *Tg(mfap4:turquoise)*$^{xt27}$ larvae was potentially confounded by luminal autofluorescence that was
191 more noticeable in CSE-exposed larvae (Figure 2B).
192
193 The enhanced effects of CSE on innate immune cell numbers in the larval gut led us to hypothesise that the
194 microbiota may interact with CSE to drive inflammation at zebrafish larval mucosal surfaces as observed
195 with other chemical irritants (31, 32). Thus, we next examined the effect of CSE and the role of changes in

196 the endogenous microbiota by depleting bacteria with broad spectrum antibiotics prior to CSE exposure
197 from 5 to 6 dpf. Antibiotic treatment did not affect the ability of 2% CSE to increase neutrophil or
198 macrophage fluorescence in the larval gut suggesting that the natural gut microbiota is not necessary to
199 drive the acute inflammatory effects of 2% CSE (Figure 3A and 3B).
200
201 Microbiota from CS-exposed mice increases the neutrophilic inflammatory effects of CSE
202 We next assessed if the microbiota of chronically CS-exposed mice could impart increases in sensitivity to
203 CSE exposure by exposing 3 dpf microbiota-depleted larval zebrafish to faecal homogenate from mice
204 exposed to CS/air controls for 10 weeks and CSE. We used the suboptimal concentration of 1% CSE, which
205 did not induce intestinal inflammation in our acute exposure assay, to detect enhancement of inflammation
206 by microbiota derived from the faeces of CS-exposed mice.
207
208 The total count of neutrophil fluorescence was unaffected in 5 dpf larvae immersed with microbiota from
209 CS- or normal air-exposed control mice, and the addition of 1% CSE (Figure 4A and 4B).
210
211 Exposure to microbiota from CS-exposed or control mice did not affect neutrophil fluorescence in the gut of
212 wild-type 5 dpf larvae compared to germ-free reared larvae (Figure 4C and 4D). Addition of 1% CSE did not
213 affect neutrophil fluorescence in the gut in 5 dpf larvae raised microbiota-depleted or in those exposed to
214 microbiota from control non-smoked mice. However, 5 dpf larvae that had been exposed to microbiota
215 from smoked mice and 1% CSE had significantly more neutrophil fluorescence in the gut than any of the
216 control groups. This pattern was replicated by *il1b* transcription levels quantified by RT-qPCR (Figure 4E).
217
218 CS-exposed mouse microbiota increases the macrophage inflammatory effects of CSE
219 Analysis of *Tg(mfap4:turquoise)*$^{xt27}$ macrophage reporter larvae revealed increased total macrophage
220 fluorescence in 5 dpf larvae that that had been exposed to microbiota from CS-exposed mice and 1% CSE
221 compared to any of the control groups, except for the air-exposed mouse microbiota and 1% CSE control
222 group (Figure 5A and 5B). Quantification of gut macrophage fluorescence was again confounded by luminal
223 autofluorescence in CSE-exposed larvae, appearing to be elevated in all CSE-exposed groups (Figure 5C and
224 5D).
225
226 **CS-exposed faecal microbiota contains culturable bacteria that do not affect inflammatory responses**
227 To investigate if any individual species of bacteria from CS-exposed mouse microbiota were able to
228 recapitulate the effects of exposure to the bulk microbiota homogenate, we recovered bacteria from the
229 homogenised CS-exposed mouse microbiota-exposed larvae onto rich LB agar. Four species were
230 subcultured to purity by passage on LB agar and genotyped by 16s sequencing as *Acinetobacter*
231 *radioresistens*, *Bacteroides vulgatus*, *Enterobacter cancerogenus*, and *Stenotrophomonas maltophilia*
232 (Supplementary File). We then screened these individual bacteria by colonising 3 dpf microbiota-depleted
233 larvae in combination with 1% CSE exposure and found no effect on total or gut leukocyte fluorescent area
234 (Figure 6).
235
236 **Discussion**
237 Here we found the immune system of zebrafish larvae is sensitive to the pro-inflammatory neutrophilic and
238 macrophage effects of CSE. Exposing zebrafish larvae to microbiota derived from the faeces of CS-exposed
239 mice demonstrate the presence of microbes (including culturable *Acinetobacter radioresistens*, *Bacteroides*
240 *vulgatus*, *Enterobacter cancerogenus*, and *Stenotrophomonas maltophilia*) or metabolites capable of
241 amplifying the inflammatory effects of CSE across species. Together, these data establish zebrafish larvae as
242 a platform for studying the environmental interactions that affect cigarette- and tobacco-induced
243 inflammatory damage.
244
245 Our finding that CSE concentrations of >2% are toxic to zebrafish larvae are in line with previous studies by
246 Alvarez *et al.* who showed larvae can survive in a solution of approximately 1% CSE and Progatzky *et al.*
247 who utilised a 1% CSE challenge with adult zebrafish (19, 21). Exposure of adult zebrafish to CSE by Alvarez
248 *et al.* demonstrated an impairment in post-amputation fin regeneration (19). Our acute wound leukocyte

249 response data adds to this observation by suggesting that increased numbers of wound-associated
250 macrophages may impede physiological regeneration in the presence of CSE.
251
252 Our data demonstrate that exposure of zebrafish larvae to 2% CSE causes an expansion of leukocytes
253 (neutrophils and macrophages) and leukocytic inflammation in the gut. Despite the increased leukocyte
254 fluorescent area, we did not observe the mass redistribution of leukocytes to the skin mucosal surfaces as
255 we have previously documented with the enterocolitis-inducing chemical irritants dextran sodium sulfate
256 and 2,4,6-trinitrobenzene sulfonic acid (31, 32). Exposure of zebrafish larvae to a dose of 1% CSE did not
257 cause detectable changes to inflammatory markers in conventionally reared larvae. Our results are
258 comparable to work using adult zebrafish that found only a subtle inflammatory response to 1% CSE
259 exposure in the gill tissue of adult zebrafish with upregulation of inflammatory gene expression but
260 decreased or unchanged immune cell infiltration in the gills depending on the length of exposure (21).
261
262 Our system of using a sub-optimal dose of 1% CSE for two days to stimulate a below measurable amount of
263 inflammation proved sensitive to positive modulation by microbiota samples from CS-exposed mouse
264 faeces. Zebrafish have been used to as hosts for trans-species microbiota transplants (33, 34), and our
265 study expands this knowledge by demonstrating sensitivity of recipient zebrafish host inflammation to a
266 microbiota-environment interaction. These proof-of-concept data suggest that zebrafish larvae may be a
267 feasible platform with which human microbiota-CS interactions can be screened to uncover potential
268 missing links in microbiota-environment interactions that appear to predispose some smokers to the
269 development of COPD (4, 9, 11).
270
271 The failure of single bacterial species that could be cultured from the guts of zebrafish to recapitulate the
272 pro-inflammatory effects of CS-exposed mouse microbiota in the context of 1% CSE co-exposure suggest
273 either the presence of multiple microbial species and/or other microbiota or factors present in the faecal
274 homogenate. This was not unexpected as the aerobic conditions of the larval zebrafish gut does not
275 facilitate sustained colonisation by some members of the mammalian microbiota (33), and our method of
276 recovering microbes on LB agar in atmospheric conditions will further bias recovery of only species present
277 at a high proportion in the gut of colonised larvae.
278
279 Recent mouse studies have demonstrated the importance of the metabolome, including short chain fatty
280 acid output, in susceptibility to smoking-induced pathology (15, 16, 35). Given the lack of butyrate
281 production found in conventionally raised zebrafish larvae (27), we think it is unlikely that exposure to
282 control mouse faecal microbiota produces anti-inflammatory short chain fatty acids as the protective
283 mechanism against 1% CSE exposure compared to the pro-inflammatory CS-exposed mouse faecal
284 microbiota. Instead, we propose that the presence of additional toxins or pro-inflammatory factors either
285 already present or produced by complex mixtures of microbes harvested from the supernatant of faecal
286 homogenates drives inflammatory responses.
287
288 The dose response effects of CSE exposure on inflammation in larval zebrafish suggest this platform could
289 be adapted for use as a screening platform to identify positive and negative regulators of inflammation
290 (36). In this study we have demonstrated the utility of a low CSE challenge to identify CS-associated
291 microbiota as factors that increase the susceptibility of zebrafish larvae to CSE-induced inflammation.
292 Follow-up studies would identify other soluble environmental factors that increase the inflammatory
293 potential of CSE. Conversely, a higher dose of 2% CSE challenge could be used as a platform to screen for
294 inhibitors of CSE-induced inflammation. Since we have recently demonstrated the sensitivity of zebrafish
295 larval inflammation to the short chain fatty acid butyrate (27), it would be interesting to determine if high
296 dose CSE-induced inflammation in zebrafish larvae can also be ameliorated by butyrate supplementation.
297
298 In summary, we have demonstrated the suitability of zebrafish larvae for studying the inflammatory effects
299 of cigarette smoke-environment interactions and show that the CS-exposed mouse gut microbiota
300 potentiates the inflammatory effects of CSE across host species.
301
302 **DATA AVAILABILITY**

Raw data is available upon reasonable request to the corresponding authors.

**ACKNOWLEDGEMENTS**

We thank other members of the Oehlers lab at the Centenary Institute for their input into this work and maintenance of the zebrafish aquarium; Dr Angela Fontaine and Sydney Cytometry for assistance with imaging; Dr Diana Quan and Ms Trixie Wang for collection of mouse faeces; Dr Kamal Dua for supervision of VM.

**FUNDING**

This work was supported by a Centenary Institute Summer Scholarship to S.M.; University of Sydney Fellowship [grant number G197581] and NSW Ministry of Health under the NSW Health Early-Mid Career Fellowships Scheme [grant number H18/31086] to S.H.O.; the NHMRC Centre of Research Excellence in Tuberculosis Control (APP1153493) to W.J.B.; NHMRC Fellowship (APP1175134) UTS, Cancer Council NSW (1157073), and the Rainbow Foundation to P.M.H.; Graduate School of Health and University of Technology Sydney (UTS President's scholarship and UTS International Research Scholarship) to V.M..

**References**

1. WHO. Tobacco 2021 [Available from: https://www.who.int/news-room/fact-sheets/detail/tobacco.
2. Jones B, Donovan C, Liu G, Gomez HM, Chimankar V, Harrison CL, et al. Animal models of COPD: What do they tell us? Respirology. 2017;22(1):21-32.
3. Keely S, Talley NJ, Hansbro PM. Pulmonary-intestinal cross-talk in mucosal inflammatory disease. Mucosal Immunol. 2012;5(1):7-18.
4. Budden KF, Gellatly SL, Wood DL, Cooper MA, Morrison M, Hugenholtz P, et al. Emerging pathogenic links between microbiota and the gut-lung axis. Nat Rev Microbiol. 2017;15(1):55-63.
5. Verschuere S, Bracke KR, Demoor T, Plantinga M, Verbrugghe P, Ferdinande L, et al. Cigarette smoking alters epithelial apoptosis and immune composition in murine GALT. Laboratory Investigation. 2011;91(7):1056-67.
6. Allais L, Kerckhof FM, Verschuere S, Bracke KR, De Smet R, Laukens D, et al. Chronic cigarette smoke exposure induces microbial and inflammatory shifts and mucin changes in the murine gut. Environmental microbiology. 2016;18(5):1352-63.
7. Wronikowska O, Michalak A, Skalicka-Woźniak K, Crawford AD, Budzyńska B. Fishing for a deeper understanding of nicotine effects using zebrafish behavioural models. Progress in Neuro-Psychopharmacology and Biological Psychiatry. 2020;98:109826.
8. Hoyt ATM, Canfield MAPD, Romitti PAPD, Botto LDMD, Anderka MTSD, Krikov SVM, et al. Associations between Maternal Periconceptional Exposure to Secondhand Tobacco Smoke and Major Birth Defects. American journal of obstetrics and gynecology. 2016;215(5):613.e1-.e11.
9. Budden KF, Shukla SD, Rehman SF, Bowerman KL, Keely S, Hugenholtz P, et al. Functional effects of the microbiota in chronic respiratory disease. Lancet Respir Med. 2019;7(10):907-20.
10. Fricker M, Goggins BJ, Mateer S, Jones B, Kim RY, Gellatly SL, et al. Chronic cigarette smoke exposure induces systemic hypoxia that drives intestinal dysfunction. JCI Insight. 2018;3(3).
11. Bowerman KL, Rehman SF, Vaughan A, Lachner N, Budden KF, Kim RY, et al. Disease-associated gut microbiome and metabolome changes in patients with chronic obstructive pulmonary disease. Nat Commun. 2020;11(1):5886.
12. Malyla V, Paudel KR, Shukla SD, Donovan C, Wadhwa R, Pickles S, et al. Recent advances in experimental animal models of lung cancer. Future Med Chem. 2020;12(7):567-70.
13. Shanahan ER, Shah A, Koloski N, Walker MM, Talley NJ, Morrison M, et al. Influence of cigarette smoking on the human duodenal mucosa-associated microbiota. Microbiome. 2018;6(1):150.
14. Pavia CS, Pierre A, Nowakowski J. Journal of medical microbiology. 2000;49(7):675-6.
15. Jang YO, Kim OH, Kim SJ, Lee SH, Yun S, Lim SE, et al. High-fiber diets attenuate emphysema development via modulation of gut microbiota and metabolism. Scientific reports. 2021;11(1):7008.

16. Jang YO, Lee SH, Choi JJ, Kim DH, Choi JM, Kang MJ, et al. Fecal microbial transplantation and a high fiber diet attenuates emphysema development by suppressing inflammation and apoptosis. Exp Mol Med. 2020;52(7):1128-39.
17. Gosens R, Hiemstra PS, Adcock IM, Bracke KR, Dickson RP, Hansbro PM, et al. Host-microbe cross-talk in the lung microenvironment: implications for understanding and treating chronic lung disease. Eur Respir J. 2020;56(2).
18. Ellis LD, Soo EC, Achenbach JC, Morash MG, Soanes KH. Use of the zebrafish larvae as a model to study cigarette smoke condensate toxicity. PLoS ONE. 2014;9(12):e115305.
19. Alvarez M, Chávez MN, Miranda M, Aedo G, Allende ML, Egaña JT. A Novel In Vivo Model to Study Impaired Tissue Regeneration Mediated by Cigarette Smoke. Scientific reports. 2018;8(1):10926.
20. Palpant NJ, Hofsteen P, Pabon L, Reinecke H, Murry CE. Cardiac Development in Zebrafish and Human Embryonic Stem Cells Is Inhibited by Exposure to Tobacco Cigarettes and E-Cigarettes. PLoS ONE. 2015;10(5):e0126259.
21. Progatzky F, Cook H, Lamb J, Bugeon L, Dallman M. Mucosal inflammation at the respiratory interface: A zebrafish model. American journal of physiology Lung cellular and molecular physiology. 2015;310:ajplung.00323.2015.
22. Massarsky A, Prasad GL, Di Giulio RT. Total particulate matter from cigarette smoke disrupts vascular development in zebrafish brain (Danio rerio). Toxicology and applied pharmacology. 2018;339:85-96.
23. Massarsky A, Jayasundara N, Glazer L, Levin ED, Prasad GL, Di Giulio RT. Outcomes of developmental exposure to total particulate matter from cigarette smoke in zebrafish (Danio rerio). Neurotoxicology. 2018;68:101-14.
24. Renshaw SA, Trede NS. A model 450 million years in the making: zebrafish and vertebrate immunity. Disease models & mechanisms. 2012;5(1):38-47.
25. Hall C, Flores MV, Storm T, Crosier K, Crosier P. The zebrafish lysozyme C promoter drives myeloid-specific expression in transgenic fish. BMC Dev Biol. 2007;7(1):42.
26. Walton EM, Cronan MR, Beerman RW, Tobin DM. The Macrophage-Specific Promoter mfap4 Allows Live, Long-Term Analysis of Macrophage Behavior during Mycobacterial Infection in Zebrafish. PLoS ONE. 2015;10(10):e0138949.
27. Cholan PM, Han A, Woodie BR, Watchon M, Kurz AR, Laird AS, et al. Conserved anti-inflammatory effects and sensing of butyrate in zebrafish. Gut Microbes. 2020;12(1):1-11.
28. Melancon E, Gomez De La Torre Canny S, Sichel S, Kelly M, Wiles TJ, Rawls JF, et al. Best practices for germ-free derivation and gnotobiotic zebrafish husbandry. Methods in cell biology. 2017;138:61-100.
29. Beckett EL, Stevens RL, Jarnicki AG, Kim RY, Hanish I, Hansbro NG, et al. A new short-term mouse model of chronic obstructive pulmonary disease identifies a role for mast cell tryptase in pathogenesis. J Allergy Clin Immunol. 2013;131(3):752-62.
30. Petzold AM, Balciunas D, Sivasubbu S, Clark KJ, Bedell VM, Westcot SE, et al. Nicotine response genetics in the zebrafish. Proc Natl Acad Sci U S A. 2009;106(44):18662-7.
31. Oehlers SH, Flores MV, Okuda KS, Hall CJ, Crosier KE, Crosier PS. A chemical enterocolitis model in zebrafish larvae that is dependent on microbiota and responsive to pharmacological agents. Dev Dyn. 2011;240(1):288-98.
32. Oehlers SH, Flores MV, Hall CJ, Crosier KE, Crosier PS. Retinoic acid suppresses intestinal mucus production and exacerbates experimental enterocolitis. Dis Model Mech. 2012;5(4):457-67.
33. Rawls JF, Mahowald MA, Ley RE, Gordon JI. Reciprocal gut microbiota transplants from zebrafish and mice to germ-free recipients reveal host habitat selection. Cell. 2006;127(2):423-33.
34. Cholan PM, Morris S, Luo K, Chen J, Boland JA, McCaughan GW, et al. Transplantation of high fat fed mouse microbiota into zebrafish embryos identifies pathobiont species. bioRxiv. 2021:2021.04.28.441900.
35. Rutting S, Xenaki D, Malouf M, Horvat JC, Wood LG, Hansbro PM, et al. Short-chain fatty acids increase TNFalpha-induced inflammation in primary human lung mesenchymal cells through the activation of p38 MAPK. American journal of physiology Lung cellular and molecular physiology. 2019;316(1):L157-L74.
36. Oehlers SH, Flores MV, Hall CJ, Wang L, Ko DC, Crosier KE, et al. A whole animal chemical screen approach to identify modifiers of intestinal neutrophilic inflammation. FEBS J. 2017;284(3):402-13.

411 **FIGURE LEGENDS**

412 **Figure 1: Cigarette smoke extract is toxic to zebrafish larvae, and causes increased embryo motility, and**
413 **greater macrophage influx into wounds**

414 A. Survival of 3 dpf larvae after exposure to CSE. Individual Log-rank comparison scores: P(0% vs 1%) =
415 0.3173, P(0% vs 2%) = 0.0798, P(0% vs 3%) <0.0001, P(1 vs 3) <0.0001, P(2% vs 3%) <0.0001. Starting n per
416 group: 0 = 45 larvae, 1% = 45 larvae, 2% = 45 larvae, 3% = 36 larvae.
417 B. Representative images of 5 dpf larvae exposed to CSE from 3 dpf. Scale bar = 1 mm.
418 C. Total distance moved in 15 minutes by 5 dpf larvae exposed to CSE from 3 dpf. Statistical comparison by
419 ANOVA, data are representative of two biological replicates.
420 D. Quantification of neutrophil fluorescent pixel area within 100 µm of the wound margin at 6 hpw in 5 dpf
421 larvae exposed to CSE from 3 dpf. Statistical comparison by ANOVA, data are normalised and combined
422 from two biological replicates.
423 E. Quantification of macrophage fluorescent pixel area within 100 µm of the wound margin at 6 hpw in 5
424 dpf larvae exposed to CSE at doses indicated from 3 dpf. Statistical comparison by ANOVA, data are
425 normalised and combined from two biological replicates.
426

427 **Figure 2: Acute exposure to CSE induces myelopoiesis in zebrafish larvae**

428 A. Representative images of 6 dpf *Tg(lyzC:DsRed)*$^{nz50}$ larvae exposed to CSE for 24 hours from 5 dpf.
429 B. Quantification of total neutrophil fluorescent pixel area in 6 dpf larva exposed to CSE for 24 hours from 5
430 dpf.
431 C. Representative images of 6 dpf *Tg(mfap4:turquoise)*$^{xt27}$ larvae exposed to CSE for 24 hours from 5 dpf.
432 D. Quantification of total macrophage fluorescent pixel area in 6 dpf larva exposed to CSE for 24 hours from
433 5 dpf.
434 A & C: Scale bars = 1 mm. Bounded area in insets are used to measure gut leukocytes in Figure 3 onwards.
435 B & D: Statistical comparison by ANOVA, data are representative of two biological replicates.
436

437 **Figure 3 Acute exposure to CSE induces an inflammatory response in the gut of zebrafish larvae**

438 A. Quantification of gut neutrophil fluorescent pixel area in 6 dpf larvae treated with broad spectrum
439 antibiotics (Abx) ampicillin and kanamycin and exposed to CSE from 5 dpf.
440 B. Quantification of gut macrophage fluorescent pixel area in 6 dpf larvae treated with broad spectrum
441 antibiotics (Abx) ampicillin and kanamycin and exposed to CSE from 5 dpf.
442 Statistical comparisons by ANOVA, data are representative of two biological replicates.
443

444 **Figure 4 CS-exposed mouse microbiota increases the neutrophilic inflammatory effects of CSE**

445 A. Representative images of 5 dpf microbiota-depleted *Tg(lyzC:DsRed)*$^{nz50}$ larvae exposed to combinations
446 of CS- or control normal air-exposed mouse microbiota with or without 1% CSE from 3 dpf.
447 B. Quantification of total neutrophil fluorescent pixel area per larva exposed to combinations of CS- or
448 control normal air-exposed mouse microbiota with or without 1% CSE from 3 dpf. Statistical comparison by
449 ANOVA, data are representative of two biological replicates.
450 C. Representative images of the posterior guts of microbiome depleted *Tg(lyzC:DsRed)*$^{nz50}$ larvae exposed to
451 combinations of CS- or control normal air-exposed mouse microbiota with or without 1% CSE from 3 dpf.
452 Area used for analysis demarcated by yellow box.
453 D. Quantification of gut neutrophil fluorescent pixel area per larva exposed to combinations of CS- or
454 control normal air-exposed mouse microbiota with or without 1% CSE from 3 dpf. Statistical comparison by
455 ANOVA, data are representative of two biological replicates.
456 E. Quantification of *il1b* transcripts by qPCR in larvae exposed to combinations of CS- or control normal air-
457 exposed mouse microbiota with or without 1% CSE from 3 dpf. Statistical comparison by ANOVA, each data
458 point represents a biological replicate with at least 10 larvae per group.
459 Scale bars = 1 mm.
460

461 **Figure 5 CS-exposed mouse microbiota increases the macrophage inflammatory effects of CSE**

462 A. Representative images of 5 dpf microbiota-depleted *Tg(mfap4:turquoise)*$^{xt27}$ larvae exposed to
463 combinations of CS- or control normal air-exposed mouse microbiota with or without 1% CSE from 3 dpf.

464 B. Quantification of total macrophage fluorescent pixel area per larva exposed to combinations of CS- or
465 control normal air-exposed mouse microbiota with or without 1% CSE. Statistical comparison by ANOVA,
466 data are representative of two biological replicates.
467 C. Representative images of the posterior guts of microbiome depleted *Tg(mfap4:turquoise)*$^{xt27}$ larvae
468 exposed to combinations of CS- or control normal air-exposed mouse microbiota with or without 1% CSE.
469 Area used for analysis demarcated by yellow box.
470 D. Quantification of gut macrophage fluorescent pixel area per larva exposed to combinations of CS- or
471 control normal air-exposed mouse microbiota with or without 1% CSE. Statistical comparison by ANOVA,
472 data are representative of two biological replicates.
473 Scale bars indicate 1 mm.
474
475 **Figure 6 CS-exposed faecal microbiota contain culturable bacteria that do not affect inflammatory**
476 **responses**
477 A. Quantification of total neutrophil fluorescent pixel area per larva exposed to bacterial isolates with or
478 without 1% CSE.
479 B. Quantification of gut neutrophil fluorescent pixel area per larva exposed to bacterial isolates with or
480 without 1% CSE.
481 C. Quantification of total macrophage fluorescent pixel area per larva exposed to bacterial isolates with or
482 without 1% CSE.
483 D. Quantification of gut macrophage fluorescent pixel area per larva exposed to bacterial isolates with or
484 without 1% CSE. Statistical comparisons by ANOVA.
485
486 **Supplementary File: Identification of isolated bacterial strains**
487 Top NCBI BLAST hit strain information and sequencing data used for BLAST.
488

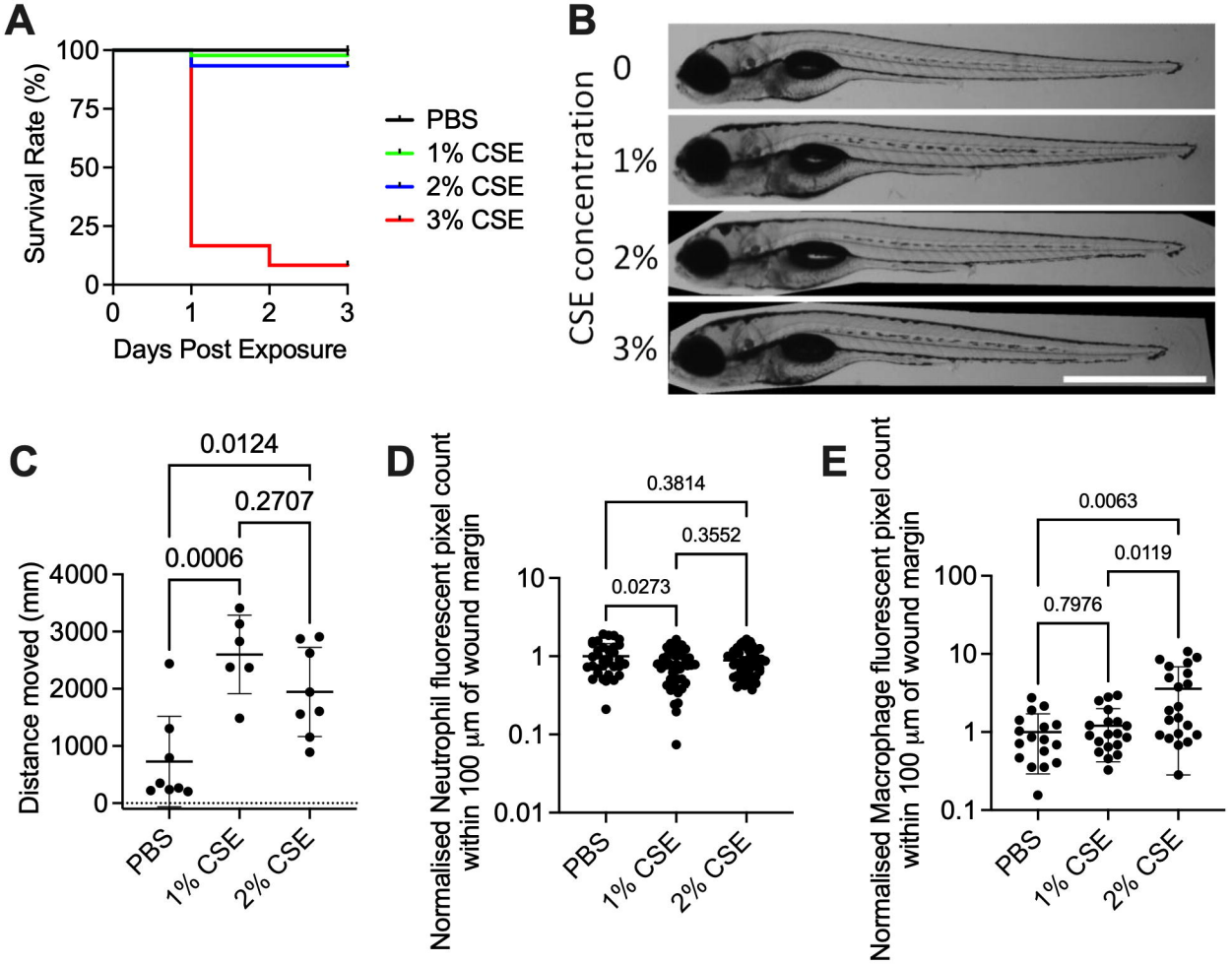
A
Survival Rate (%)
100
75
50
25
0
0
1
2
3
Days Post Exposure
PBS
1% CSE
2% CSE
3% CSE
B
CSE concentration
0
1%
2%
3%
C
0.0124
0.2707
0.0006
Distance moved (mm)
4000
3000
2000
1000
0
PBS
1% CSE
2% CSE
D
0.3814
0.3552
0.0273
Normalised Neutrophil fluorescent pixel count within 100 μm of wound margin
10
1
0.1
0.01
PBS
1% CSE
2% CSE
E
0.0063
0.0119
0.7976
Normalised Macrophage fluorescent pixel count within 100 μm of wound margin
100
10
1
0.1
PBS
1% CSE
2% CSE

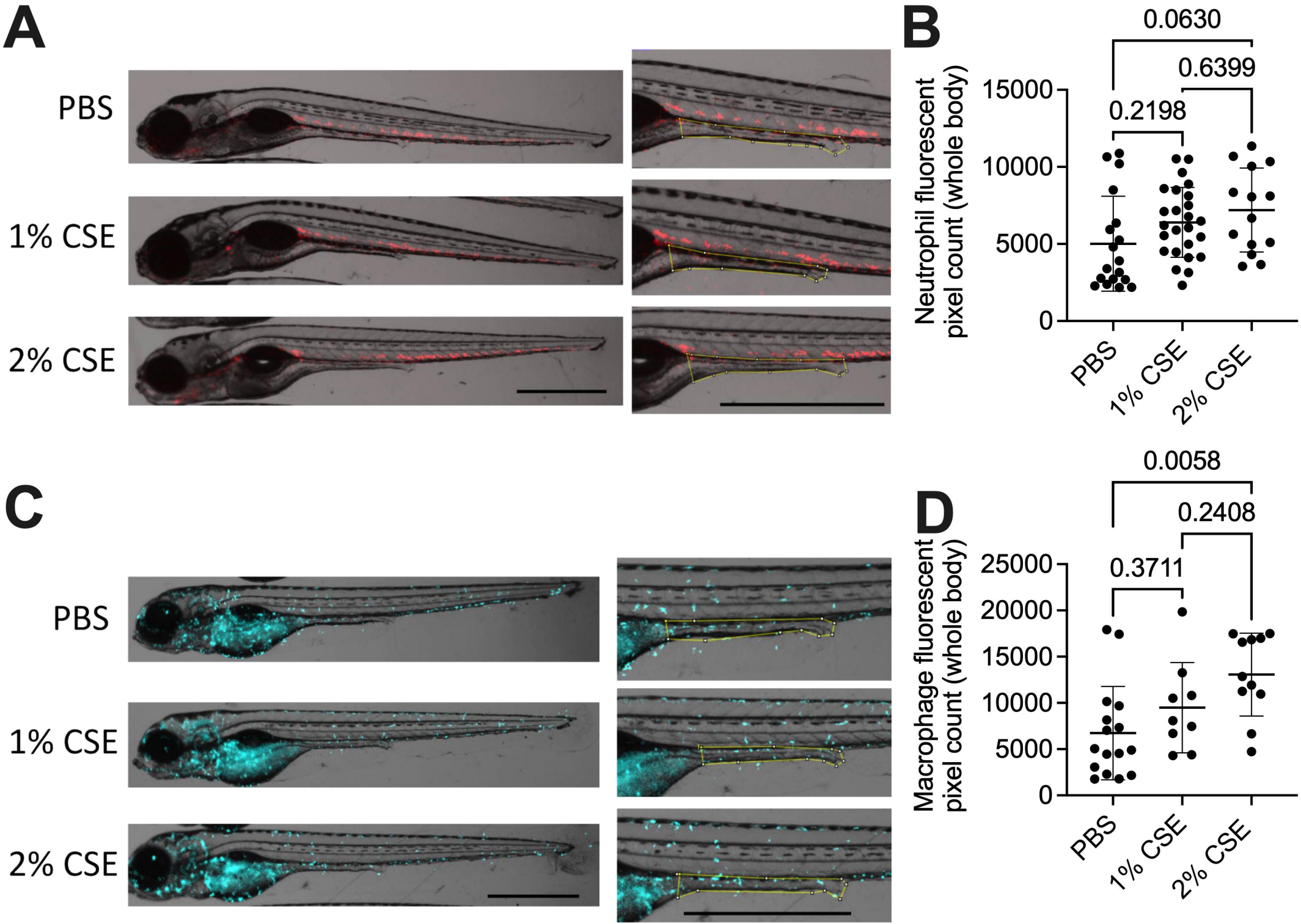
A
PBS
1% CSE
2% CSE
B
0.0630
0.6399
0.2198
Neutrophil fluorescent pixel count (whole body)
15000
10000
5000
0
PBS
1% CSE
2% CSE
C
PBS
1% CSE
2% CSE
D
0.0058
0.2408
0.3711
Macrophage fluorescent pixel count (whole body)
25000
20000
15000
10000
5000
0
PBS
1% CSE
2% CSE

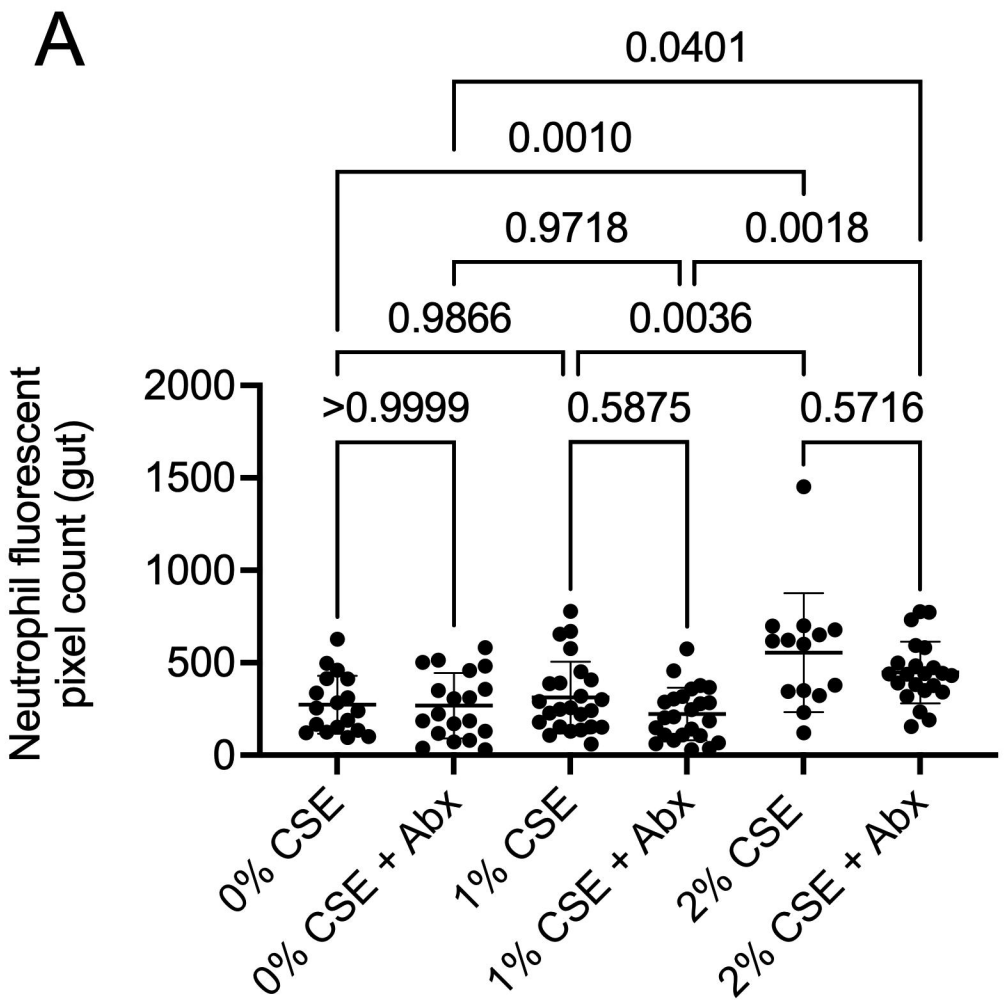
A
0.0401
0.0010
0.9718
0.0018
0.9866
0.0036
>0.9999
0.5875
0.5716
Neutrophil fluorescent pixel count (gut)
2000
1500
1000
500
0
0% CSE
0% CSE + Abx
1% CSE
1% CSE + Abx
2% CSE
2% CSE + Abx

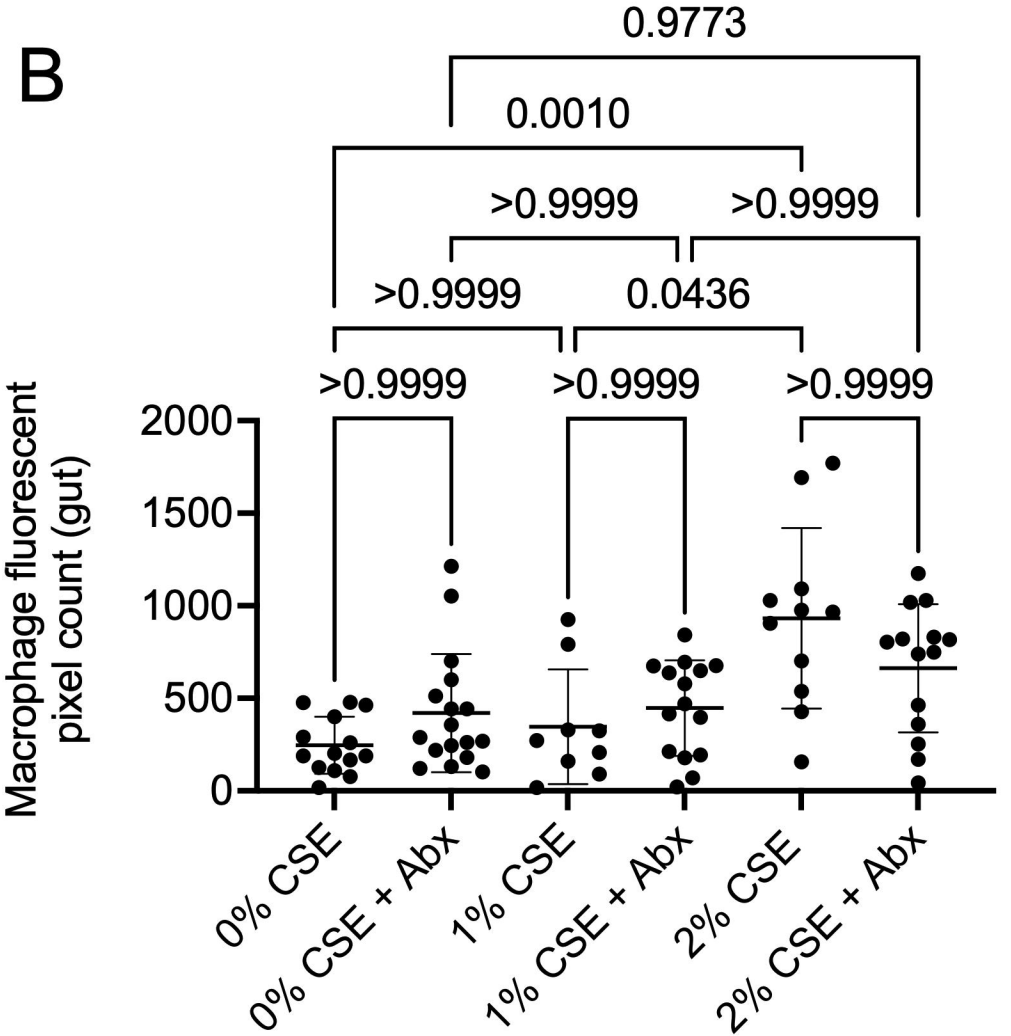
B
0.9773
0.0010
>0.9999
>0.9999
>0.9999
0.0436
>0.9999
>0.9999
>0.9999
Macrophage fluorescent pixel count (gut)
2000
1500
1000
500
0
0% CSE
0% CSE + Abx
1% CSE
1% CSE + Abx
2% CSE
2% CSE + Abx

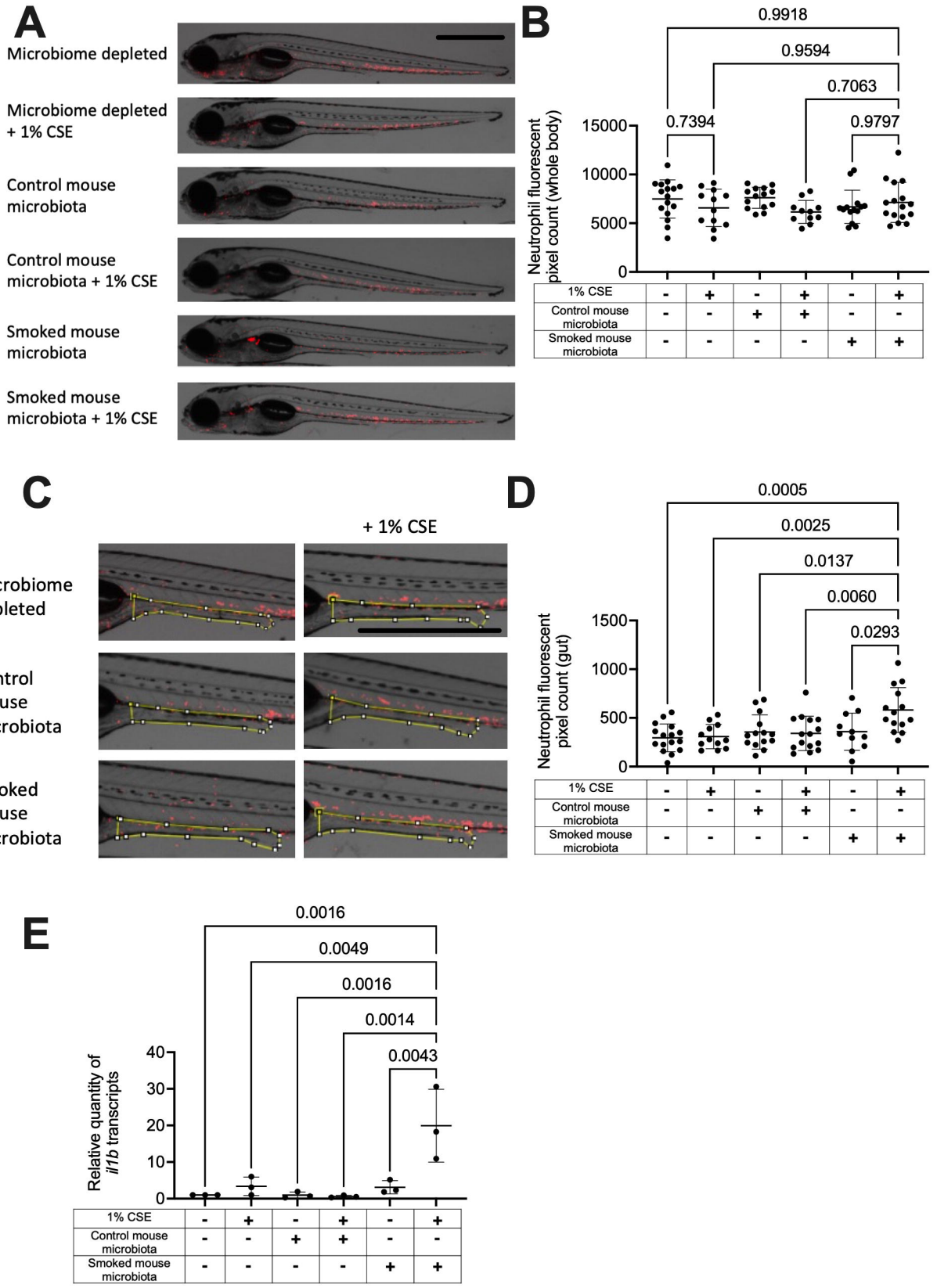
A
Microbiome depleted
Microbiome depleted + 1% CSE
Control mouse microbiota
Control mouse microbiota + 1% CSE
Smoked mouse microbiota
Smoked mouse microbiota + 1% CSE
B
0.9918
0.9594
0.7063
0.7394
0.9797
Neutrophil fluorescent pixel count (whole body)
15000
10000
5000
0
1% CSE
Control mouse microbiota
Smoked mouse microbiota
C
+ 1% CSE
Microbiome depleted
Control mouse microbiota
Smoked mouse microbiota
D
0.0005
0.0025
0.0137
0.0060
0.0293
Neutrophil fluorescent pixel count (gut)
1500
1000
500
0
1% CSE
Control mouse microbiota
Smoked mouse microbiota
E
0.0016
0.0049
0.0016
0.0014
0.0043
Relative quantity of il1b transcripts
40
30
20
10
0
1% CSE
Control mouse microbiota
Smoked mouse microbiota

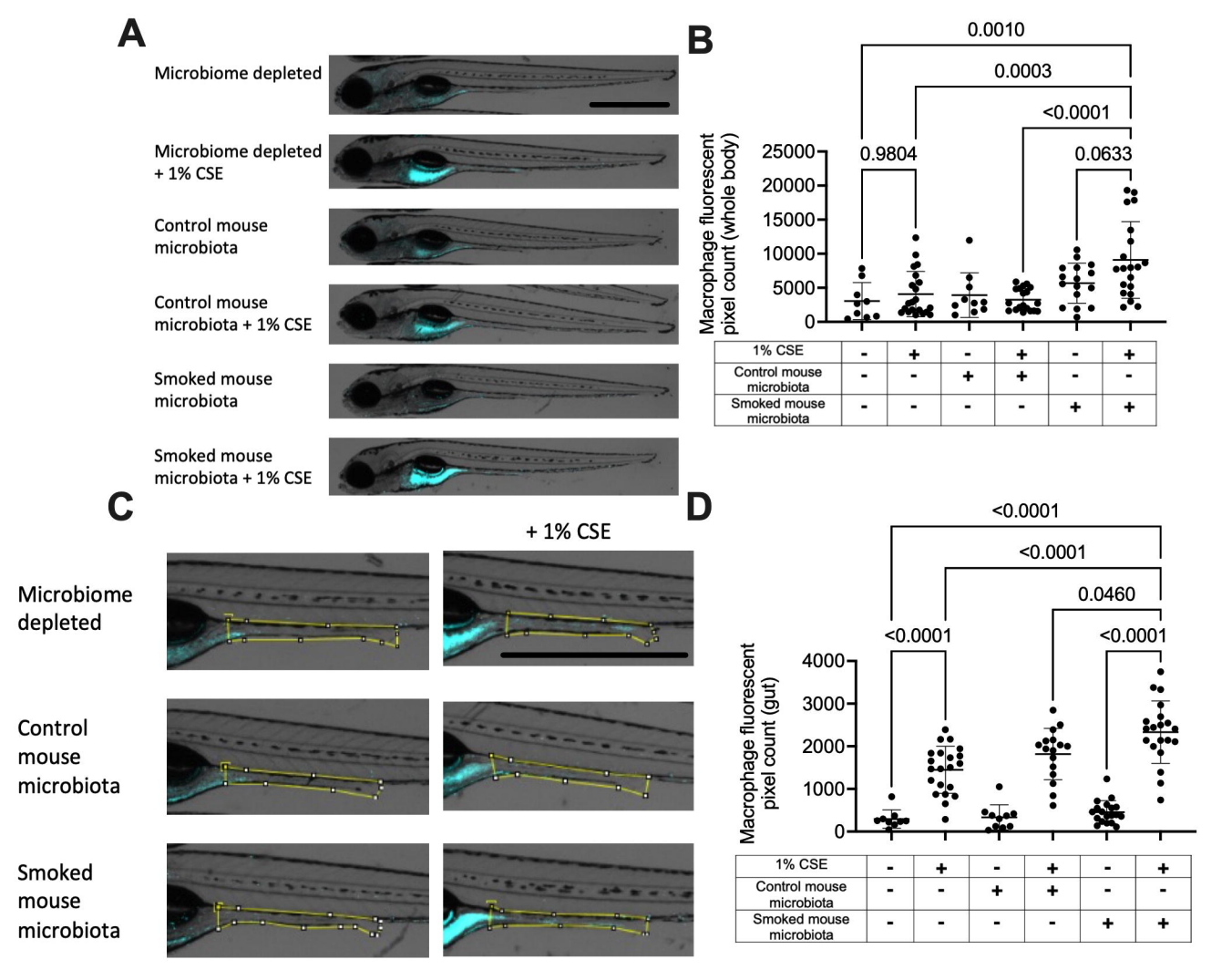
A
Microbiome depleted
Microbiome depleted + 1% CSE
Control mouse microbiota
Control mouse microbiota + 1% CSE
Smoked mouse microbiota
Smoked mouse microbiota + 1% CSE
B
Macrophage fluorescent pixel count (whole body)
25000
20000
15000
10000
5000
0
0.0010
0.0003
<0.0001
0.9804
0.0633
1% CSE
Control mouse microbiota
Smoked mouse microbiota
C
+ 1% CSE
Microbiome depleted
Control mouse microbiota
Smoked mouse microbiota
D
Macrophage fluorescent pixel count (gut)
4000
3000
2000
1000
0
<0.0001
<0.0001
0.0460
<0.0001
<0.0001
1% CSE
Control mouse microbiota
Smoked mouse microbiota

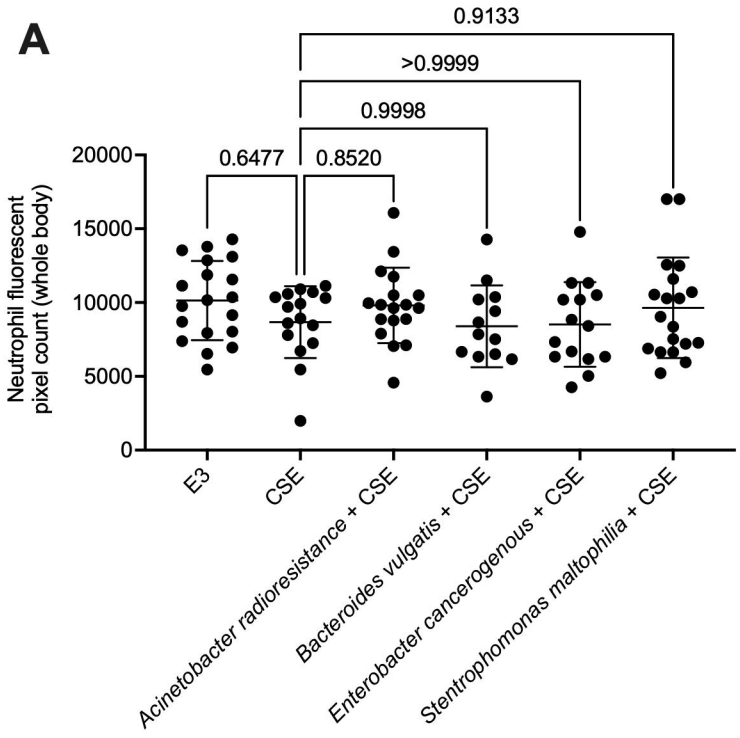
A
0.9133
>0.9999
0.9998
0.6477
0.8520
20000
15000
10000
5000
0
Neutrophil fluorescent pixel count (whole body)
E3
CSE
Acinetobacter radioresistance + CSE
Bacteroides vulgatis + CSE
Enterobacter cancerogenous + CSE
Stentrophomonas maltophilia + CSE

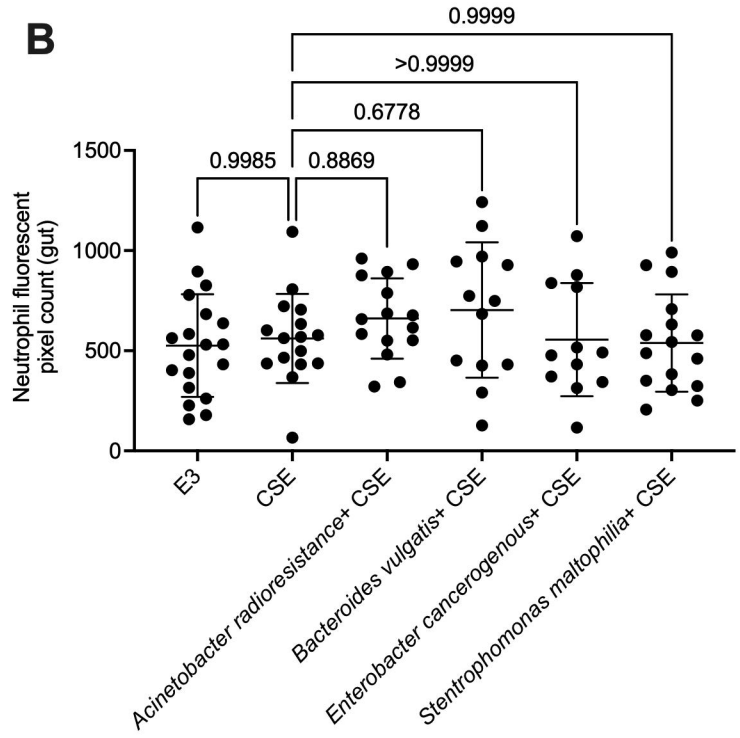
B
0.9999
>0.9999
0.6778
0.9985
0.8869
1500
1000
500
0
Neutrophil fluorescent pixel count (gut)
E3
CSE
Acinetobacter radioresistance+ CSE
Bacteroides vulgatis+ CSE
Enterobacter cancerogenous+ CSE
Stentrophomonas maltophilia+ CSE

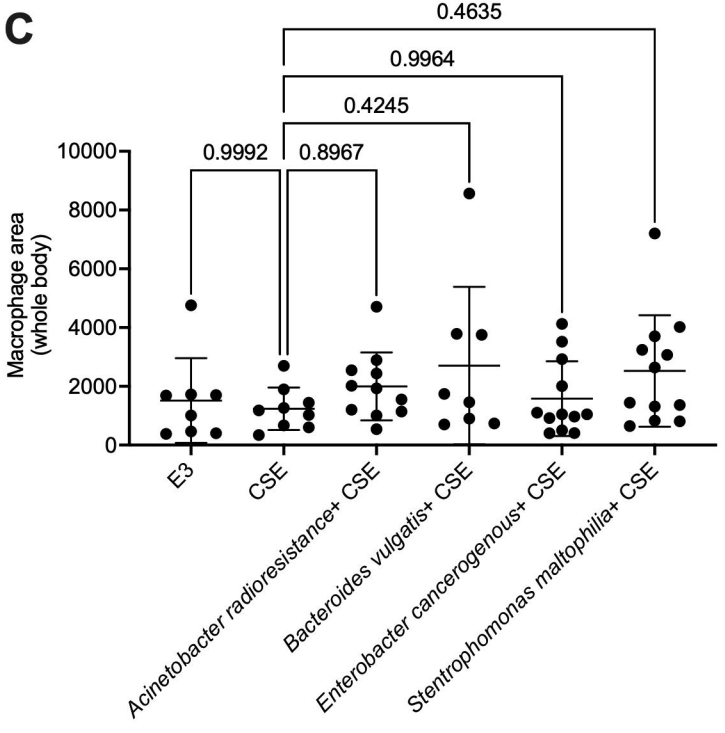
C
0.4635
0.9964
0.4245
0.9992
0.8967
10000
8000
6000
4000
2000
0
Macrophage area (whole body)
E3
CSE
Acinetobacter radioresistance+ CSE
Bacteroides vulgatis+ CSE
Enterobacter cancerogenous+ CSE
Stentrophomonas maltophilia+ CSE

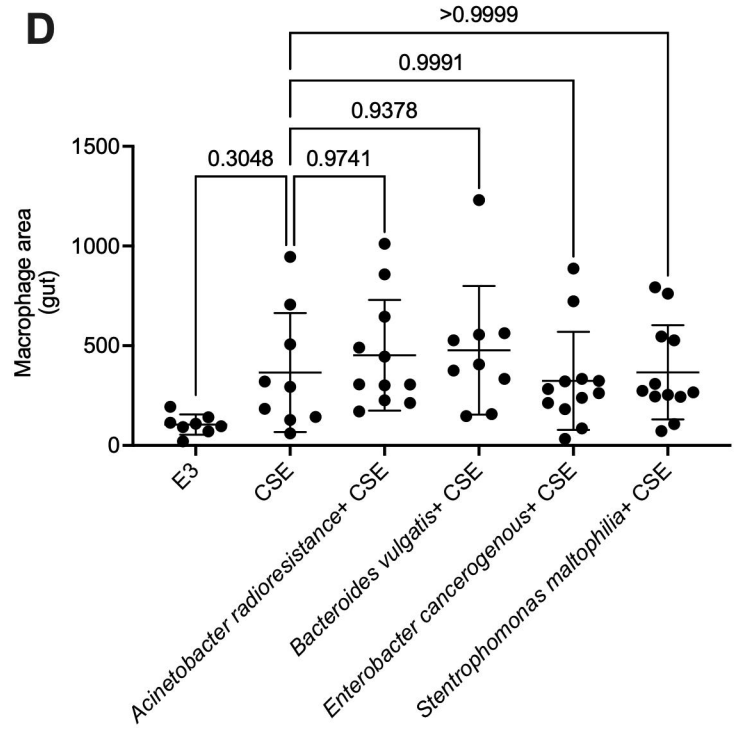
D
>0.9999
0.9991
0.9378
0.3048
0.9741
1500
1000
500
0
Macrophage area (gut)
E3
CSE
Acinetobacter radioresistance+ CSE
Bacteroides vulgatis+ CSE
Enterobacter cancerogenous+ CSE
Stentrophomonas maltophilia+ CSE